Carbohydrate Polymers 82 (2010) 46–53

Contents lists available at ScienceDirect

Carbohydrate Polymers

journal homepage: www.elsevier.com/locate/carbpol

Diffusion and viscosity in arabinoxylan solutions: Implications for nutrition

Kinnari J. Shelat[a], Francisco Vilaplana[a], Timothy M. Nicholson[b], Kok Hou Wong[a], Michael J. Gidley[a], Robert G. Gilbert[a,*]

[a] The University of Queensland, Centre for Nutrition & Food Sciences, School of Land Crop & Food Sciences, Brisbane, Qld 4072, Australia
[b] The University of Queensland, Centre for High Performance Polymers, School of Chemical Engineering, Brisbane, Qld 4072, Australia

ARTICLE INFO

Article history:
Received 15 February 2010
Accepted 12 April 2010
Available online 18 April 2010

Keywords:
Arabinoxylan
Non-starch polysaccharide
Viscosity
Diffusion
Digestion
Size-exclusion chromatography

ABSTRACT

Non-starch polysaccharides such as arabinoxylans have important roles in the human diet, resulting in potential benefits such as increased microbial fermentation, promotion of beneficial microflora, prevention of re-absorption of bile acids leading to lower plasma cholesterol, and retardation of starch digestion. The latter two beneficial effects may arise from viscosity and/or diffusion phenomena in the gastrointestinal tract. To study this, measurements of the viscosity and diffusion coefficients of a polymer probe similar in size to both bile salt micelles and alpha-amylase were carried out for water solutions of three arabinoxylans with differing viscosities. Diffusion coefficients were obtained using fluorescence recovery after photobleaching (FRAP). The concentration dependence of both viscosity and diffusion coefficients followed the usual behaviour of polymers for each of three arabinoxylan samples. However, at a given concentration, the sample with the highest viscosity also had the highest probe diffusion coefficient: the reverse of what would be expected for homogeneous solutions. This apparent anomaly is ascribed to differences in polymer structure between the three samples giving rise to varying levels of local polymer aggregation and consequent microvoids. These differences are verified using characterisation with multiple-detection size-exclusion chromatography. Deviations from simple Stokes–Einstein behaviour are ascribed to the existence of aggregates in solution. The results show that studies of the role of arabinoxylans in human nutrition cannot assume that the diffusion coefficients of species with sizes in the range important for digestive processes in a series of samples will increase with decreasing viscosity at a given concentration: diffusion coefficient and viscosity must be measured independently.

1. Introduction

Cereal grains, important for human nutrition, mainly consist of starch and protein together with non-starch polysaccharides (NSPs). These NSPs are major component of cell walls, particularly in the starchy endosperm (Saulnier, Guillon, Sado, & Rouau, 2007, Saulnier, Sado, Branlard, Charmet, & Guillon, 2007). Although NSPs typically represent only about 3–8% of the total of the grain, they have major effects on the technological use and nutritional value of cereal grains due to their hydration properties, viscosity in aqueous solution, and consequent role as dietary fibre. Arabinoxylan (AX) is the major NSP of wheat endosperm cell walls and shows quantitative differences in structural features depending on tissue location as well as grain species (Saulnier, Guillon, et al., 2007; Saulnier, Sado, et al., 2007). AX is a copolymer with a linear backbone of (1–4)-linked β-D-xylopyranosyl units; these β-D-xylopyranosyl units are substituted at some O_2 and/or O_3 positions with α-L-arabinofuranose. Some of these arabinofuranose units are esterified with ferulic acid, with the consequent potential for oxidative cross-linking. Diverse physicochemical properties, particularly solubility and network formation, can result from variation in the level and pattern of arabinose substitution and the extent of cross-linking via ferulic acid substituents (Saulnier, Guillon, et al., 2007; Saulnier, Sado, et al., 2007).

The structure of AX, its physicochemical properties, and its role in food quality and beneficial health effects, have received some attention in the literature (Hoffmann, Kamerling, & Vliegenthart, 1992; Izydorczyk & Biliaderis, 1992, 1995; Knudsen & Jorgensen, 2007; Pitkanen, Virkki, Tenkanen, & Tuomainen, 2009; Saulnier, Guillon, et al., 2007; Saulnier, Sado, et al., 2007; Warrand et al., 2005). AX is a recognised dietary fibre, and has been reported to lower cholesterol absorption, to improve metabolic control in type 2 diabetes subjects, and to increase microbial fermentation and promote microbial flora in the large intestine (Hanai et al., 1997; Lopez et al., 1999; Lu, Walker, Muir, & Dea, 2004). Despite this importance, AXs are considerably less studied than other NSPs such as (1,3;1,4)-β-D-glucan ('β-glucan') and guar galactomannan. Blackburn and Johnson (1981) and Jenkins et al. (1978) measured changes in the

* Corresponding author. Tel.: +61 7 3365 4809; fax: +61 7 3365 1188.
E-mail address: b.gilbert@uq.edu.au (R.G. Gilbert).

0144-8617/$ – see front matter © 2010 Elsevier Ltd. All rights reserved.
doi:10.1016/j.carbpol.2010.04.019

viscosity of gastrointestinal contents of rats in the presence of guar galactomannan and inferred that the presence of this soluble dietary fibre reduces absorption of glucose from the small intestine because it causes viscosity to increase. The principal hypotheses for the reduced glycemic response in the presence of soluble fibres are delayed gastric emptying, a lower rate of diffusion of alpha-amylase to starch substrates and of released hydolysed starch fragments from the intestinal lumen to the absorptive epithelial cells that line the digestive tract and/or increased intestinal mobility resulting in faster intestinal passage (Dikeman & Fahey, 2006; Jenkins et al., 1978; Lu et al., 2004). These mechanisms are considered to be the result of either the highly viscous nature of soluble fibres in aqueous solution and/or the effect on the diffusion of digestive enzymes in the presence of viscous dietary fibres in the gut. Although the presence of soluble dietary fibre in food is likely to alter the physical state of intestinal contents, particularly increasing the viscosity, it is not yet established whether there is a simple relationship between bulk viscosity and the diffusion of probe molecules of the size of bile salt micelles and alpha-amylase for solutions of soluble dietary fibres such as AX.

The present investigation describes the rheological and diffusion behaviour of solutions of three AX samples from wheat and rye sources. Both viscosity and diffusion effects are measured as a function of AX concentration. The diffusion coefficients of an enzyme-sized probe (FITC–dextran) in AX solutions are measured using fluorescence recovery after photobleaching (FRAP) (Axelrod, Koppel, Schlessinger, Elson, & Webb, 1976; Bryers & Drummond, 1998; Burke, Park, Srinivasarao, & Khan, 2000; Perry, Fitzgerald, & Gilbert, 2006), an optical-microscopy technique. The rheological behaviour of the AXs is characterised in water and in water–dextran solution. A series of experiments using both steady and oscillatory shear in Couette geometry are performed. In addition, the molecular size and weight distributions in dimethyl sulfoxide solution, and the average size of AX molecules/aggregates in aqueous solution, are obtained using size-exclusion chromatography (SEC; also known as gel-permeation chromatography, GPC) and dynamic light scattering, respectively. The objective of the size distribution analysis is to see if there are significant differences between the structure and/or chemical heterogeneity in three samples of AX, and that of the dynamic light scattering is to see if the average size depends on AX concentration, which would indicate aggregation.

2. Materials and methods

2.1. Materials

Three AXs, with kinematic viscosity at 1% (w/v) concentration reported by the manufacturer to be 24, 29 and 33 cSt (corresponding to dynamic viscosities of 24, 29 and 33 mPa s; 1 cP = 1 mPa s for a fluid of density 1 g cm^{-3}) were procured from Megazyme International Ireland Ltd. We denote these here as AX24 (WAX-MV, lot 20401), AX29 (WAX-MV, lot 40301) and AX33 (RAX-HV, lot 20601). AX24 and AX29 are from wheat and AX33 is from rye. These materials have recently been characterised (Pitkanen et al., 2009), including chemical composition analysis by NMR spectroscopy and molecular size analysis by size-exclusion chromatography (SEC) in 0.1 M $NaNO_3$ in water, and 0.01 M LiBr in dimethyl sulfoxide. Fluorescein isothiocyanate conjugate tagged dextrans (FITC–dextran) of weight-average molecular weight 7.0×10^4, denoted FD70S, was obtained from Sigma Chemical Co. and used as received. This probe was chosen due to size similarities with digestive enzymes such as α-amylase (crystallographic radius of ~3 nm, Payan et al., 1980) as well as bile salt micelles (typically ~10 nm diameter, Carey & Small, 1970). FD70S contained 0.003–0.02 mol of FITC per mol of glucose and had a stated dispersity (this term replacing what used to be denoted by terms such as 'polydispersity' or 'polydispersity index', Gilbert et al., 2009) ($\bar{M}_w/\bar{M}_n$) < 1.30. The hydrodynamic radius of the probe was 6 nm (Burke et al., 2000; Perry et al., 2006; Pluen, Netti, Jain, & Berk, 1999).

2.2. Measurement of diffusion coefficients using FRAP

The method used was similar to that used for the measurement of diffusion coefficient of FITC–dextran in starch solutions by Perry et al. (2006) 0.7% (w/v) solution of FITC–dextran in deionised (DI) water was prepared by dissolving FITC–dextran in DI water at ambient temperature. The sample for FRAP was prepared by dissolving AX (at concentrations ranging from 0.025% to 1%, w/v) in FITC–dextran/DI water solution at 40 °C, using 300 rpm over 1–2 h in a thermomixer (Eppendorf AG 22331, Hamburg, Germany). The sample was introduced into the cavity of a microscope glass slide using a micropipette (38–40 μL) and the glass slide was covered with a cover slip using liquid nail polish. FRAP experiments were carried out with a ZEISS LSM 510 META Confocal Microscope using a 10× objective lens. The uniform bleach disc radius was ~25 μm and samples were bleached using a 10 mW argon ion laser. FRAP image acquisition was performed using frame size 256 × 256 with maximum scan speed. The bleaching of the sample was ~40–50% after the first two scans. The numerical aperture and depth range were the same as described by Perry et al. (2006); the temperature was ambient (~23 °C). Data were fitted using the model of Braeckmans for the normalised recovery curve at time t, $F_{tot}(t)/F_0$ (Braeckmans, Peeters, Sanders, De Smedt, & Demeester, 2003):

$$\frac{F_{tot}(t)}{F_0} = 1 + [1 - e^{-2y}(I_0(2y) + I_1(2y))]\sum_{n=0}^{\infty}\left[\frac{(-K_0)^n}{n!}\frac{1}{\sqrt{1+n}}\right] \quad (1)$$

where $y = \omega^2/(4Dt)$, D is the two-dimensional lateral diffusion coefficient, ω is the e^{-2} radius of the Gaussian bleach spot, I_0 and I_1 are the modified Bessel functions of the zero and first order, respectively, and K_0 an instrumental parameter. The fit to the data involves least-squares minimisation with respect to the quantities D and K_0.

2.3. Rheological characteristics of arabinoxylan

Rheological studies were performed with an Advanced Rheometric Expansion System (ARES; TA Instruments). Solutions at different concentrations, ranging from 0.2% (w/v) to 10% (w/v), were prepared by dissolving AX29 and AX33 in DI water at 80 °C for 2 h; rheology was not performed on AX24 because of limited sample availability. Further samples were prepared by dissolving AXs in a 0.7% (w/v) dextran/water solution. Steady-shear and oscillatory measurements were carried out over a range of frequencies using strain control with both Couette and parallel plate geometries. All the samples were first tested in oscillatory mode to determine their linear viscoelastic region by performing a strain sweep experiment at a frequency of 10 rad s^{-1}. This then allowed for a suitable choice of strain amplitude to be employed for frequency sweep experiments from 0.1 to 100 rad s^{-1}. The steady-shear experiments were performed for a range of frequencies from 0.5 to 100 s^{-1}. All the samples were freshly prepared for each measurement and all the measurements were performed in duplicate at 23 °C.

2.4. SEC

The three different AX samples were injected into an Agilent 1100 Series SEC system (PSS GmbH. Mainz, Germany) using a GRAM preColumn and two 100 columns (PSS GmbH. Mainz, Germany) in series, in a column oven at 80 °C. The flow rate was 0.3 mL min^{-1}. The system was equipped with multi-angle laser light scattering

(MALLS) (BIC-MwA7000, Brookhaven Instrument Corp., New York, USA) followed by parallel flow into a refractive index detector (RID) (Shimadzu RID-10A, Shimadzu Corp., Japan) and a viscometric detector (ETA-2010, PSS GmbH, Mainz, Germany). The AX concentration used was 2 mg/mL.

Calibration was with pullulan standards (PSS GmbH, Mainz, Germany), with a molecular weight range of 342–1.66×10^6. SEC separates by a size parameter, hydrodynamic volume, V_h. AX has numerous monosaccharide branches, and like any complex branched polymer, there is no direct relation between size and molecular weight. Data are therefore reported in terms of V_h; to aid intuition, in the present case the data are presented equivalently in terms of the corresponding hydrodynamic radius R_h, with $V_h = 4/3\pi R_h^3$. The upper limit of the size of the standards corresponds to $\log R_h/\text{nm} \sim 1.65$, or $R_h \sim 45$ nm.

The Mark–Houwink parameters for pullulan in DMSO/LiBr (0.5 wt%) at 80 °C are $K = 2.427 \times 10^{-4}$ dL g^{-1} and $\alpha = 0.6804$ (Cave, Seabrook, Gidley, & Gilbert, 2009). The method for calibration to obtain V_h has been given elsewhere (Cave et al., 2009).

2.5. Average size measurement

The average size measurement of 'particles' (individual polymer molecules and any aggregates) in AX solutions was performed using a Malvern Zetasizer Nano ZS. This device uses dynamic light scattering at a backscattering angle of 173° to give an average size (which we denote the Zetasizer-average size), which can be meaningfully compared across similar samples. It is noted that this average size has no simple relation to an average radius of gyration of molecules in a polymer solution, and depends on the chain dynamics (both local motions and translational diffusion) of the polymer in the sample (Galinsky & Burchard, 1997). For polydisperse samples, such as the present, the inversion of scattering data cannot give a unique size distribution.

The average particle size was measured for all AX samples over the concentration range of 0.0125–1% (w/v). The AX solutions were freshly prepared following the same procedure as described above. Each measurement was performed in triplicate and an average taken of the three measurements.

3. Results and discussions

3.1. Diffusion coefficients

Fig. 1 shows an example of a normalised fluorescence recovery curve of FITC–dextran in AX solution for AX29 at 0.5% (w/v) concentration. The continuous line shows the fitting to Eq. (1); a similarly good fit was obtained in all cases. The values of D as a function of concentration for AX24, AX29 and AX33 are shown in Fig. 2. The highest concentration of AX studied was 1% by weight; higher concentrations are very viscous and so present difficulties in loading into the cavity of the microscope slide used for FRAP measurements. As expected, the diffusion coefficients of each of the AXs decrease with increasing solution concentration and thus increasing viscosity, but the AX with the higher supplier-reported viscosity at 1% (w/v) shows a *higher* diffusion coefficient. This is the opposite from what would be expected from simple Stokes–Einstein behaviour which predicts that probe diffusion should be higher for lower viscosity solutions.

3.2. Rheology

All FRAP measurements involved the presence of significant amounts of fluorophore-labelled dextran, which might affect the rheology compared to the same system without dextran. Fig. 3 shows a comparison between steady-shear viscosities of AX29

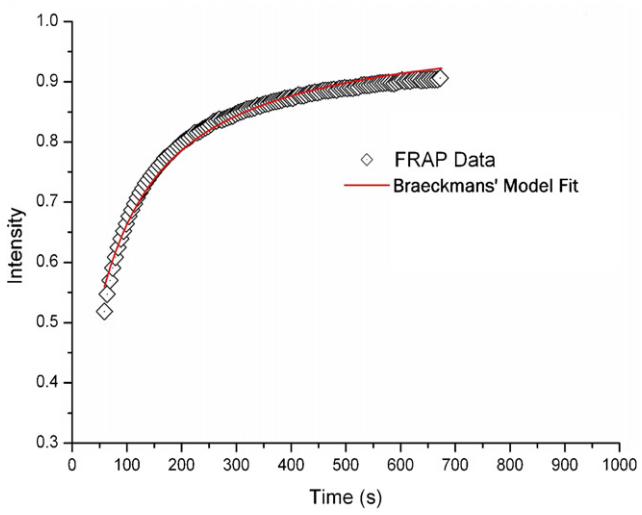

Fig. 1. Example of normalised intensity vs. time curve for AX29 at 0.5% (w/v) concentration in a FRAP experiment. Following bleaching of a defined area, fluorescence intensity recovers by diffusion of fluorescent FITC–dextran into the bleached area. Data fitting using the Braeckmans model (Eq. (1)) is shown.

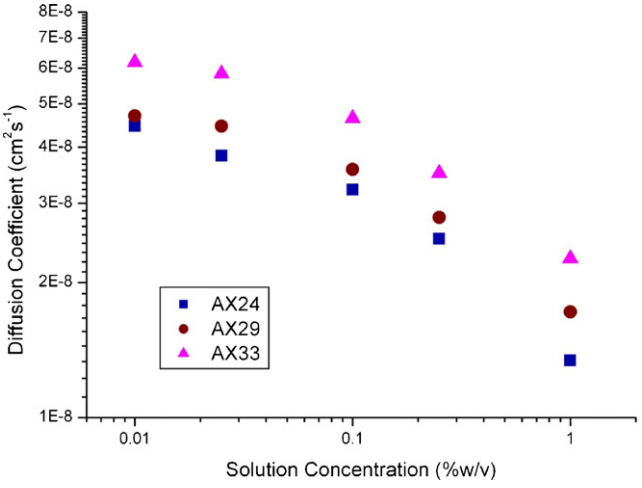

Fig. 2. Diffusion coefficients as function of concentration for AXs of three different viscosities.

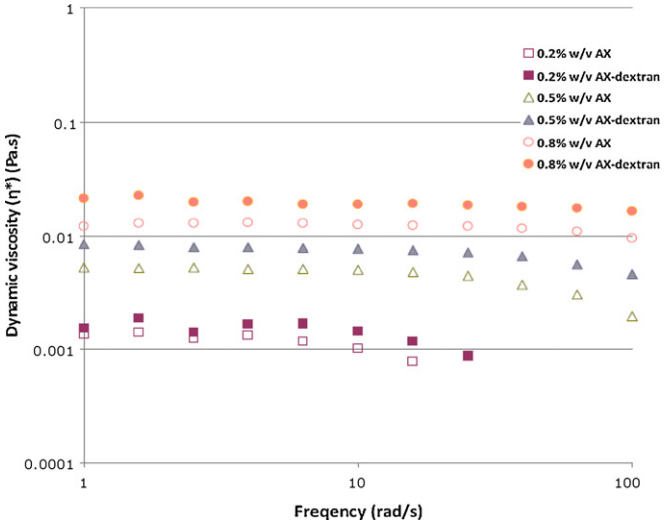

Fig. 3. Dynamic viscosity as a function of frequency for AX29 at various concentrations in water (open symbols) and in 0.7% (w/v) dextran/water solution (closed symbols).

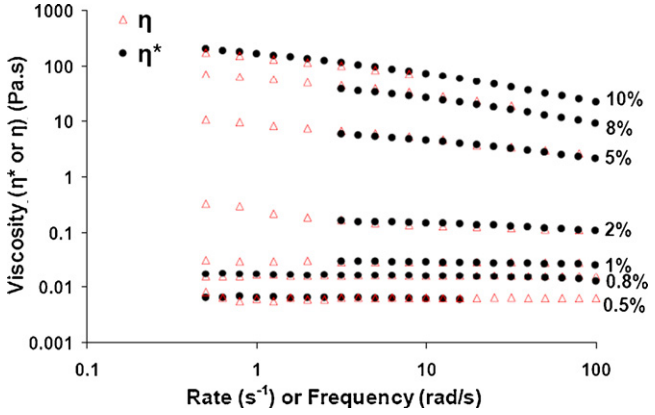

Fig. 4. Oscillatory (η^*) and steady-state (η) viscosity of AX33 solutions at different concentrations in water (open symbols) and in 0.7% (w/v) dextran/water solution (closed symbols).

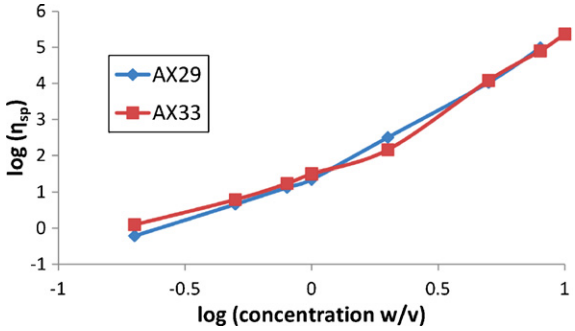

Fig. 6. Specific viscosity as a function of concentration for AX29 and AX33 in aqueous solution.

in water and in 0.7% (w/v) dextran/water. The addition of dextran increases the viscosity by approximately 50% regardless of AX concentration. This variation is smaller than the increase in viscosity seen between the different AX concentrations studied, so the results from the wider range of AX concentrations in water solution are thus representative of the behaviour in dextran/water and may be compared to the diffusion results.

Fig. 4 shows measured dynamic (η^*) and steady-state viscosities (η) as a function of frequency and shear rate for AX33. Similar results with lower absolute values were obtained for AX29. It is apparent that these solutions obey the empirical Cox-Merz rule (the values of $\eta(\dot{\gamma})$ and $\eta^*(\omega)$ are superposable), which suggests that the system does not have any complex long-range structure (Wissbrun & Dealy, 1999). The zero-shear viscosity (i.e. the plateau viscosity as frequency tends to zero) is clearly visible for the lower concentration solutions. The onset of shear thinning moves to lower shear rates as the concentration increases, and for the higher concentrations the zero-shear viscosity was estimated by the values at the lowest shear for which acceptable measurements could be made. The measured values at 1% concentration of the steady-shear viscosities at low shear are 24 and 31 mPa s for the two samples whose viscosities are quoted by the manufacturer as 29 and 33 mPa s. This difference is not of significance.

Fig. 5 shows dynamic storage (G') and loss (G'') moduli for AX33. Similar behaviour was seen for AX29. It was observed that in both AX samples, both moduli increase with an increase in the frequency. At lower concentrations the values of G'' are higher than those of G', indicating a dominant viscous behaviour in the system. As the concentration increases, the presence of a cross-over point of G' and G'' is observed which shifts to lower frequencies with further increase in the concentration. Lazaridou, Biliaderis, Micha-Screttas, and Steele (2004) observed similar behaviour in the case of another NSP, β-glucan, and this is a typical characteristic of macromolecular solutions or of dispersions with topological entanglement.

In general, for a range of random coil polymers, there is a critical overlap concentration (c^*) at which the transition from dilute to concentrated solution behaviour occurs. However, departures from this have been observed in certain systems, ascribed to specific intermolecular association or hyperentanglements (Morris, Cutler, Ross-Murphy, & Rees, 1981). In the present study, as shown in Fig. 6, in the double log plot of specific viscosity, $(\eta/\eta_s)-1$ (where η_s = viscosity of pure solvent), versus concentration, there is no sharp c^*; this behaviour is typical of polydisperse polymer solutions. Also, at higher concentration (>1%, w/v and above the apparent c^* value), the slope of the double log plot is ~4.5 and ~4.1 for AX33 and AX29, respectively, suggesting intermolecular association ('hyperentanglement') in these polysaccharide solutions (Morris et al., 1981). Such hyperentanglement may result in, or be the consequence of, polymer aggregation. Aggregation of AXs in dimethyl sulfoxide and water/salt solutions has also been observed by Pitkanen et al. (2009).

3.3. Correlation between diffusion and viscosity measurements

As shown in Fig. 7, for a given polymer (AX 29 or AX 33), the measured diffusion coefficients for a given sample decrease with increasing zero-shear viscosity, as expected from the Stokes–Einstein relation for hard spheres:

$$D = \frac{k_B T}{6\pi\eta R} \quad (2)$$

Here k_B is the Boltzmann constant, T the absolute temperature, D the diffusion coefficient, R the hard-sphere radius of the probe and η the zero-shear viscosity of the continuous phase (in this case

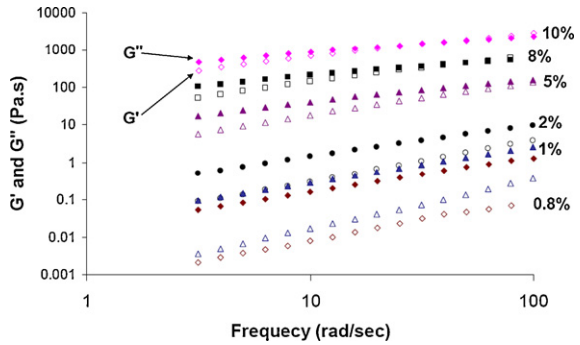

Fig. 5. Storage (G') (open symbols) and loss (G'') (closed symbols) moduli for AX33 solutions at different concentrations.

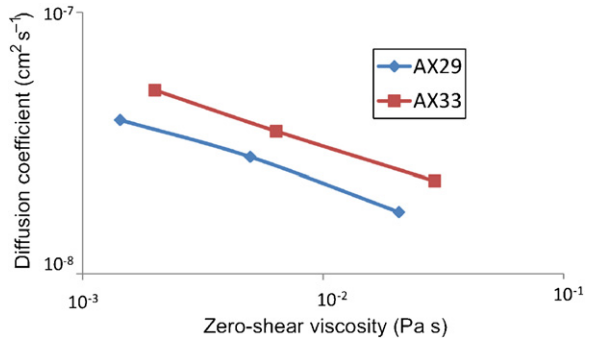

Fig. 7. Diffusion coefficients as a function of zero-shear viscosity of the polymer solution for two AX samples for concentrations 0.2%, 0.5% and 1% (w/v).

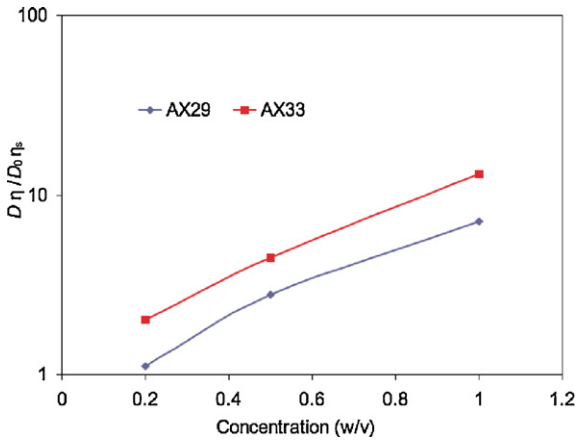

Fig. 8. Diffusion coefficients as a function of AX29 and AX33 concentration plotted against a dimensionless quantity that would be unity at all concentrations if the Stokes–Einstein relation were obeyed: $D\eta/D_0\eta_0$ (see text).

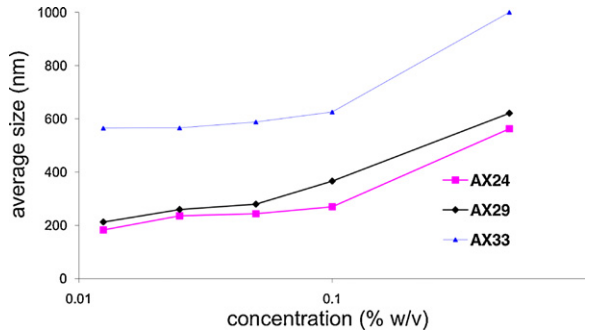

Fig. 9. Zetasizer-average sizes for AX24, AX29, and AX33 in water at different concentrations.

the solution of AX). Qualitatively, the behaviour for a given AX is as expected, with a decreasing diffusivity corresponding to an increase in viscosity; however the higher viscosity AX33 displays an *increased* diffusivity compared to the lower viscosity AX 29.

A quantitative deviation from Stokes–Einstein behaviour can be seen by plotting the data as $D\eta/D_0\eta_s$, where D_0 is the diffusion coefficient of the FITC–dextran probe alone, the value of which was obtained from extrapolation of diffusion data to zero AX concentration and η_s is the viscosity of the dextran solution. This is shown in Fig. 8. Won, Onyenemezu, Miller, and Lodge (1994) defined positive and negative deviations from the Stokes–Einstein relationship (Eq. (2)) as $D\eta/D_0\eta_s > 1$ and <1, respectively. These deviations were explained in terms of the probe experiencing a local microviscosity which differs from the bulk viscosity, where the microviscosity is that calculated from the diffusivity using the Stokes–Einstein relationship. A positive deviation corresponds to a diffusivity that decreases less rapidly than the viscosity increases as the concentration rises, which would be interpreted as a microviscosity being less than the bulk viscosity. Marginal positive or negative deviations from Stokes–Einstein behaviour have been observed in the past in different types of polymeric systems (Alvarez-Mancenido et al., 2006; De Smedt et al., 1997; Jena & Bloomfield, 2005; Lin & Phillies, 1984; Lin & Phillles, 1982; Won et al., 1994).

Fig. 8 displays an increasing positive deviation from Stokes–Einstein behaviour as the concentration increases. This can be interpreted as a decrease in the microviscosity experienced by the probe. This in turn could arise from either a reduction in the hydrodynamic radius of the probe, or to a reduction in the friction experienced with the bulk (solution of AX). A reduction in hydrodynamic volume would result from an interaction between the probe and the AX which increases as concentration increases, whilst a reduction in friction could arise from an aggregation of the AX molecules, thus reducing the local concentration experienced by the probe in non-aggregated 'microvoid' regions.

As was noted above, the diffusion coefficients for the two different polymers, AX29 and AX 33, *increase* with increasing 1% (w/v) bulk viscosity, over the whole concentration range examined. Further, Fig. 8 shows that the higher molecular weight AX shows a greater positive deviation from Stokes–Einstein behaviour. Again this can be interpreted as a decrease in microviscosity promoted by intermolecular interactions of the polysaccharide. Pitkanen et al. (2009) characterised a range of wheat and rye AX samples, and observed distinct differences in the substitution patterns for wheat and rye AXs, although overall arabinose to xylose ratios were similar. In rye arabinoxylan (e.g. AX 33), the number of α-L-Araf substituents linked to mono-substituted β-D-Xylp units was higher than α-L-Araf residues in di-substituted xylopyranosyl units. In contrast, for wheat arabinoxylan (e.g. AX 29), the number of α-L-Araf substituents linked to di-substituted xylopyranosyl units was higher. If di-substituted xylose units prevent aggregation and mono-substituted units are tolerated in aggregate junction zones, this difference in the substitution pattern may facilitate higher aggregation in AX33 solution compared to that of AX29. Increasing aggregation would create more microvoids and hence a lower microviscosity resulting in a higher probe diffusion coefficient.

3.4. Aggregation and particle size of arabinoxylan

The Zetasizer-average sizes of different viscosity AXs as functions of concentration in water are shown in Fig. 9. Due to instrumental limitations, size measurements were performed on relatively dilute solutions, with samples ranging from 0.0125% (w/v) to 0.5% (w/v) AX. As predicted from diffusion and viscosity measurements above, larger particles are detected for polymers with the higher 1% (w/v) viscosities. There is also an increase in average size with increase in concentration for all AX samples, with this increase more pronounced above 0.1% (w/v). Moreover, molecular sizes in DMSO are ~101 nm whereas the Zetasizer particle sizes in water are an order of magnitude larger, immediately suggesting significant aggregation in water.

Pitkanen et al. (2009) also found that the particle size of AX33 was higher than that of AX24 in 0.1 M $NaNO_3$. This suggests that aqueous AX systems contain aggregates, with the size of the aggregates increasing with concentration, and varying with AX substitution patterns. The reduced microviscosity between these aggregates may therefore provide the explanation for the positive deviation from Stokes–Einstein behaviour shown above.

3.5. Characterisation by multiple-detection size-exclusion chromatography (SEC)

The arabinoxylan samples were analysed with SEC using DMSO-based systems to promote molecular solubility and limit/prevent aggregation. The three detectors (viscometric, differential refractive index, DRI, and multi-angle laser light scattering, MALLS) give three independent distributions/functions of size: the number distribution $N(V_h)$, the SEC weight distribution $w(\log V_h)$ and the size dependence of the weight-average molecular weight, $\bar{M}_w(V_h)$, respectively. The same data can also be used to obtain the size dependence of the number-average weight, $\bar{M}_n(V_h)$; note that any three of these four are independent, while the fourth can be derived from the others. The MALLS data also yield the V_h dependence of the radius of gyration, R_g. Three representations of the data are given here; Fig. 10 gives $w(\log V_h)$ and $R_g(V_h)$, and Fig. 11 gives the size dependences of the two average molecular weights. The

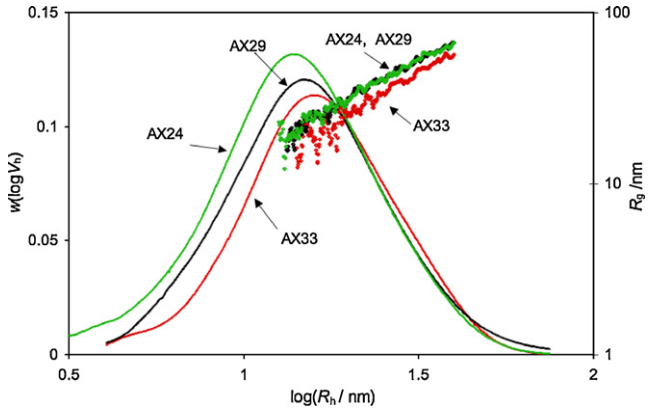

Fig. 10. SEC distributions, $w(\log V_h)$, and $R_g(V_h)$, in terms of hydrodynamic radius, for solutions of AX24, AX29 and AX33 in DMSO containing 0.5 wt% LiBr. The R_h values for AX24 and AX29 are superposable within experimental uncertainty.

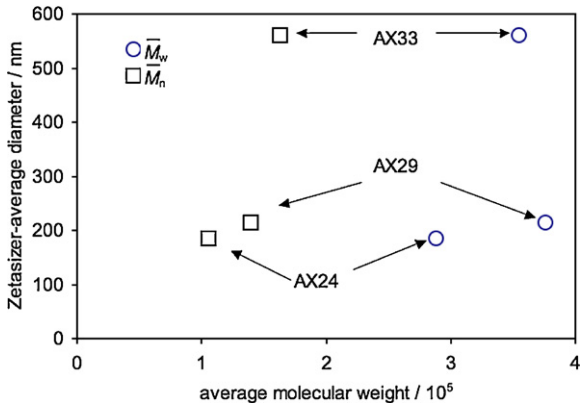

Fig. 12. Dependence of the overall number- and weight-average molecular weights from SEC in DMSO containing 0.5 wt% LiBr on the Zetasizer-average sizes at 0.0125% in water for each AX.

values of R_h above the size limit of the standards used are only semi-quantitative.

The $\bar{M}_n(V_h)$ data require viscometric and DRI data and the assumption of universal calibration (Grubisic, Rempp, & Benoit, 1967). On the other hand, $\bar{M}_w(V_h)$ requires MALLS, DRI and also the value of the differential refractive index (dn/dc) for the polymer and solvent. These last data are not available for AX, and the $\bar{M}_w(V_h)$ given here were obtained by assuming the same values as for pullulan; the $\bar{M}_w$ results will be only semi-quantitative, and are actually values relative to pullulan.

The calculated overall molar mass averages ($\bar{M}_n$ and $\bar{M}_w$) from SEC are presented in Fig. 12, as functions of the Zetasizer-average particle sizes of each AX at the lowest concentration measured (Fig. 9). The average molar mass values are similar to those previously reported by other authors (Pitkanen et al., 2009; Sternemalm, Höije, & Gatenholm, 2008). It would be expected that higher molecular weight correlates with higher particle size; however, AX29 and AX33 have similar total molecular weights but very different sizes. This behaviour is also seen in the size dependence of the average molecular weights shown in Fig. 11. This is strongly suggestive of significant differences in branching structure and/or chemical heterogeneity.

All size distributions, $w(\log V_h)$, are similar for the three arabinoxylan samples, with the highest viscosity sample (AX33) showing more molecules of larger size, with the reverse for the lowest viscosity sample, AX24; this is as expected (Fig. 10). However, the $\bar{M}_w(V_h)$ distribution for the arabinoxylan samples (Fig. 11) shows interesting features, since sample AX33 (which was the sample with higher distribution of molecules of larger size) exhibits lower $\bar{M}_w$ values at a certain size (V_h) than the other samples (AX24 and AX29). This effect may be related to structural differences among the samples, or in this case, different substitution patterns of α-L-Araf in the β-D-Xylp backbone. Indeed, sample AX33 from rye has been reported to have mainly mono-substituted β-D-Xylp units, whereas wheat arabinoxylans (samples AX24 and AX29) exhibit higher ratio of α-L-Araf substituents linked to di-substituted xylopyranosyl units (Pitkanen et al., 2009). This closed-packing structure of α-L-Araf substituents in di-substituted β-D-Xylp units may explain why the average-weight molecular weight at a certain size is larger for wheat arabinoxylans than for rye arabinoxylan. It is worth mentioning that while the dispersity $\bar{M}_w/\bar{M}_n$ of a polymer can never be less than unity, apparent dispersities less than unity ($\bar{M}_w(V_h) < \bar{M}_n(V_h)$) are observed in the data in Fig. 11 for sample AX33 close to the limit of calibration for SEC. This is obviously an artefact in the MALLS signal caused by the low concentrations at this range of sizes during SEC separation and/or the fact that these $\bar{M}_w$ values are relative to pullulan, not absolute values.

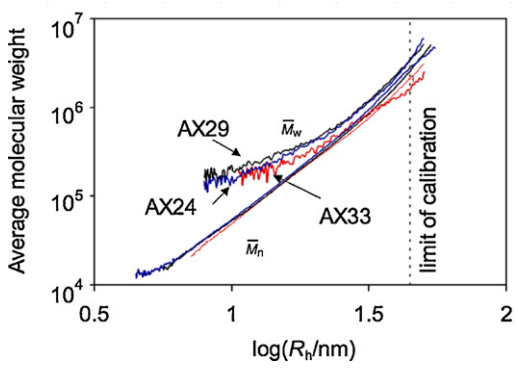

Fig. 11. Size dependences of the number- and weight-average molecular weights, $\bar{M}_n(V_h)$ and $\bar{M}_w(V_h)$, for solutions of AX24, AX29 and AX33 in DMSO containing 0.5 wt% LiBr. The $\bar{M}_n(V_h)$ for each AX is indistinguishable within experimental uncertainty. The upper limit of the calibration range of the standards is also indicated. The $\bar{M}_w(V_h)$ values are relative to starch and are only semi-quantitative.

The radii of gyration (Fig. 10) show higher values for wheat arabinoxylan samples (AX24 and AX29) than for rye arabinoxylan (AX33), indicating structural differences between the samples in terms of substitution pattern. The molecular weight dependence of the radius of gyration provides additional information about the conformational state of the macromolecules in solution, also known as fractal dimensions (Burchard, 1999). For monodisperse polymers, this dependence is well described by a simple power expression, the de Gennes scaling law concept (de Gennes, 1979):

$$R_g = K_g(\bar{M}_w)^{\nu_g} \quad (3)$$

Here K_g is a constant depending on the monomer structure and the nature of the solvent, and ν_g is an exponent which depends on the polymer architecture, temperature, and polymer–solvent interactions (ν_g = 0.5–0.6 corresponds to a linear random coil conformation in solution; ν_g = 0.33 for a sphere; and ν_g = 1 for a rod). Although deviations from this power law behaviour have been reported for complex branched polysaccharides such as glycogen or amylopectin (Rolland-Sabaté, Mendez-Montealvo, Colonna, & Planchot, 2008), a good linear correlation in the bi-logarithmic plot of R_g versus $\bar{M}_w$ was observed for the three arabinoxylan samples (plots not shown). The values of ν_g are 0.58 for rye arabinoxylan, indicating a random coil conformation in solution, whereas the coefficients for wheat arabinoxylans are significantly lower (0.45–0.47), characteristic of a more compact conformation. Similar results have been reported (Warrand et al., 2005) for constitutive arabinoxylans from flaxseeds in aqueous system (water and

$LiNO_3$), with values of ν_g ranging between 0.35 and 0.55. These results confirm the structural differences between the wheat and rye arabinoxylan samples in terms of substitution pattern, and they may provide a structural explanation for the differences in aggregation behaviour in water consistent with mono-substituted but not di-substituted xylose residues being tolerated in aggregate structures. Rye arabinoxylans with mainly mono-substituted units may be prone to adopt a random coil conformation, which would be more favourable to intermolecular interactions than a compact "branched-type" conformation preferably adopted by wheat arabinoxylans with mainly di-substituted xylose residues. These favourable intermolecular interactions in random coil conformations may be responsible for the higher capacity for supramolecular aggregation observed in rye arabinoxylan, and therefore influencing the rheological and diffusional properties. Although the conformational behaviour is reported here for a dimethyl sulfoxide-based solvent system, which is expected to act as a better solvent for arabinoxylans than water, the structural and conformational features may be compared to similar results reported by Warrand et al. (2005) for an aqueous system, to explain the supramolecular aggregation behaviour of the arabinoxylan samples in water.

4. Conclusions

The rheology and diffusion data show that these arabinoxylan solutions deviate from Stokes–Einstein behaviour in two ways: (i) an increase in the product of diffusion coefficient and viscosity with increasing polymer concentration above that predicted by the Stokes–Einstein relation, and (ii) samples with different viscosities at a given concentration showing decreasing diffusion coefficient with decreasing viscosity, the opposite of what is expected from the Stokes–Einstein relation. These comparisons reflect differences between the AX samples, as for a given sample, the diffusion coefficient of the dextran probe decreased with increasing concentration, as expected. The size measurement and rheology results confirmed the presence of variable size aggregates and of entanglements in the polysaccharide solution. The size and molecular weight data also indicate differences in branching structure and/or chemical heterogeneity. The deviation from Stokes–Einstein behaviour in (i) is the cumulative result of differences in microviscosity and macroviscosity of AX solutions due to variable size aggregates present in the solution. For (ii), the unexpected behaviour can be explained in terms of differing aggregation behaviour in AXs of different molecular substitution patterns, i.e. differences in branching structure and/or chemical heterogeneity.

This has significant implications in nutrition. The beneficial effects of non-starch polysaccharides have a number of possible origins, which include increased bowel viscosity and decreased diffusive rates of enzymes and bile salt micelles. The explanation for these effects has in the past been a single one of increasing viscosity also resulting in decreased diffusion rates of bile salt micelles and enzymes (Dikeman & Fahey, 2006; Jenkins et al., 1978). The present study shows that viscosity and diffusion are not simply related: a non-starch polysaccharide solution which has a higher viscosity than that of another may in fact have higher diffusion rates of enzymes, contrary to simple Stokes–Einstein expectations. Despite what is commonly assumed, viscosity alone may well not be the only factor in the beneficial effects of non-starch polysaccharides in human nutrition.

Acknowledgements

Funding was made available from the Australian Flagship Collaborative Research Program, provided to the High Fibre Grains Cluster via the Food Futures Flagship. FV would like to acknowledge the support of a postdoctoral fellowship from the Knut and Alice Wallenberg Foundation (Sweden). We appreciate the assistance of Anastasia Aufort in the size measurements, and thank Torsten Witt and Dr. Richard Cave for their help in SEC measurements.

References

Alvarez-Mancenido, F., Braeckmans, K., De Smedt, S. C., Demeester, J., Landin, M., & Martinez-Pacheco, R. (2006). Characterization of diffusion of macromolecules in konjac glucomannan solutions and gels by fluorescence recovery after photobleaching technique. *International Journal of Pharmaceutics*, *316*, 37–46.

Axelrod, D., Koppel, D. E., Schlessinger, J., Elson, E., & Webb, W. W. (1976). Mobility measurement by analysis of fluorescence photobleaching recovery kinetics. *Biophysical Journal*, *16*, 1055–1069.

Blackburn, N. A., & Johnson, I. T. (1981). The effect of guar gum on the viscosity of the gastrointestinal contents and on glucose uptake from the perfused jejunum in the rat. *British Journal of Nutrition*, *46*, 239–246.

Braeckmans, K., Peeters, L., Sanders, N. N., De Smedt, S. C., & Demeester, J. (2003). Three-dimensional fluorescence recovery after photobleaching with the confocal scanning laser microscope. *Biophysical Journal*, *85*, 2240–2252.

Bryers, J. D., & Drummond, F. (1998). Local macromolecule diffusion coefficients in structurally non-uniform bacterial biofilms using fluorescence recovery after photobleaching (FRAP). *Biotechnology and Bioengineering*, *60*, 462–473.

Burchard, W. (1999). Solution properties of branched macromolecules. *Advances in Polymer Science*, *143*, 113–194.

Burke, M. D., Park, J. O., Srinivasarao, M., & Khan, S. A. (2000). Diffusion of macromolecules in polymer solutions and gels: A laser scanning confocal microscopy study. *Macromolecules*, *33*, 7500–7507.

Carey, M. C., & Small, D. M. (1970). The characteristics of mixed micellar solutions with particular reference to bile. *American Journal of Medicine*, *49*, 590–608.

Cave, R. A., Seabrook, S. A., Gidley, M. J., & Gilbert, R. G. (2009). Characterization of starch by size-exclusion chromatography: The limitations imposed by shear scission. *Biomacromolecules*, *10*, 2245–2253.

de Gennes, P.-G. (1979). *Scaling concepts in polymer physics*. Ithaca, NY: Cornell University.

De Smedt, S. C., Meyvis, T. K. L., Demeester, J., Van Oostveldt, P., Blonk, J. C. G., & Hennink, W. E. (1997). Diffusion of macromolecules in dextran methacrylate solutions and gels as studied by confocal scanning laser microscopy. *Macromolecules*, *30*, 4863–4870.

Dikeman, C. L., & Fahey, G. C. (2006). Viscosity as related to dietary fiber: A review. *Critical Reviews in Food Science and Nutrition*, *46*, 649–663.

Galinsky, G., & Burchard, W. (1997). Starch fractions as examples for nonrandomly branched macromolecules. 4. Angular dependence in dynamic light scattering. *Macromolecules*, *30*, 6966–6973.

Gilbert, R. G., Hess, M., Jenkins, A. D., Jones, R. G., Kratochvil, P., & Stepto, R. F. T. (2009). Dispersity in polymer science (IUPAC recommendations 2009). *Pure and Applied Chemistry*, *81*, 351–353.

Grubisic, Z., Rempp, P., & Benoit, H. (1967). Universal calibration for gel permeation chromatography. *Journal of Polymer Science: Polymer Letters Edition*, *5*, 753–759.

Hanai, H., Ikuma, M., Sato, Y., Iida, T., Hosoda, Y., Matsushita, I., et al. (1997). Long-term effects of water-soluble corn bran hemicellulose on glucose tolerance in obese and non-obese patients: Improved insulin sensitivity and glucose metabolism in obese subjects. *Bioscience, Biotechnology, and Biochemistry*, *61*, 1358–1361.

Hoffmann, R. A., Kamerling, J. P., & Vliegenthart, J. F. G. (1992). Structural features of a water-soluble arabinoxylan from the endosperm of wheat. *Carbohydrate Research*, *226*, 303–311.

Izydorczyk, M. S., & Biliaderis, C. G. (1992). Effect of molecular size on physical properties of wheat arabinoxylan. *Journal of Agricultural and Food Chemistry*, *40*, 561–568.

Izydorczyk, M. S., & Biliaderis, C. G. (1995). Cereal arabinoxylans: Advances in structure and physicochemical properties. *Carbohydrate Polymers*, *28*, 33–48.

Jena, S. S., & Bloomfield, V. A. (2005). Probe diffusion in concentrated polyelectrolyte solutions: Effect of background interactions on competition between electrostatic and viscous forces. *Macromolecules*, *38*, 10551–10556.

Jenkins, D. J. A., Wolever, T. M. S., Leeds, A. R., Gassull, M. A., Haisman, P., Dilawari, J., et al. (1978). Dietary fibres, fibre analogues, and glucose tolerance: Importance of viscosity. *British Medical Journal*, *1*, 1392–1394.

Knudsen, K. E. B., & Jorgensen, H. (2007). Impact of wheat and oat polysaccharides provided as rolls on the digestion and absorption processes in the small intestine of pigs. *Journal of the Science of Food and Agriculture*, *87*, 2399–2408.

Lazaridou, A., Biliaderis, C. G., Micha-Screttas, M., & Steele, B. R. (2004). A comparative study on structure–function relations of mixed-linkage $(1 \rightarrow 3)$, $(1 \rightarrow 4)$ linear beta-D-glucans. *Food Hydrocolloids*, *18*, 837–855.

Lin, T.-H., & Phillies, G. D. J. (1984). Probe diffusion in polyacrylic acid:water—Effect of polymer molecular weight. *Journal of Colloid and Interface Science*, *100*, 82.

Lin, T.-H., & Phillles, G. D. J. (1982). Translational diffusion coefficient of a macroparticulate probe species in salt-free poly(acrylic acid)-water. *Journal of Physical Chemistry*, *86*, 4073–4077.

Lopez, H. W., Levrat, M.-A., Guy, C., Messager, A., Demigne, C., & Remesy, C. (1999). Effects of soluble corn bran arabinoxylans on cecal digestion, lipid metabolism, and mineral balance (Ca, Mg) in rats. *Journal of Nutritional Biochemistry*, *10*, 500–509.

Lu, Z., Walker, K., Muir, J., & Dea, K. O. (2004). Arabinoxylan fibre improves metabolic control in people with type II diabetes. *European Journal of Clinical Nutrition*, *58*, 621–628.

Morris, E. R., Cutler, A. N., Ross-Murphy, S. B., & Rees, D. A. (1981). Concentration and shear rate dependence of viscosity in random coil polysaccharide solutions. *Carbohydrate Polymers*, *1*, 5–21.

Payan, F., Haser, R., Pierrot, M., Frey, M., Astier, J. P., Abadie, B., et al. (1980). The three-dimensional structure of alpha-amylase from porcine pancreas at 5 Å resolution—The active-site location. *Acta Crystallographica Section B*, *B36*, 416–421.

Perry, P. A., Fitzgerald, M. A., & Gilbert, R. G. (2006). Fluorescence recovery after photobleaching as a probe of diffusion in starch systems. *Biomacromolecules*, *7*, 521–530.

Pitkanen, L., Virkki, L., Tenkanen, M., & Tuomainen, P. (2009). Comprehensive multi-detector HPSEC study on solution properties of cereal arabinoxylans in aqueous and DMSO solutions. *Biomacromolecules*, *10*, 1962–1969.

Pluen, A., Netti, P. A., Jain, R. K., & Berk, D. A. (1999). Diffusion of macromolecules in agarose gels: Comparison of linear and globular configurations. *Biophysical Journal*, *77*, 542–552.

Rolland-Sabaté, A., Mendez-Montealvo, M. G., Colonna, P., & Planchot, V. (2008). Online determination of structural properties and observation of deviations from power law behavior. *Biomacromolecules*, *9*, 1719–1730.

Saulnier, L., Guillon, F., Sado, P.-E., & Rouau, X. (2007). Plant cell wall polysaccharides in storage organs: Xylans (food application). In J. Kamerling, G.-J. Boons, Y. Lee, T. A. Suzuki, N. Taniguchi, & A. G. J. Voragen (Eds.), *Comprehensive glycoscience*. Amsterdam, The Netherlands: Elsevier.

Saulnier, L., Sado, P.-E., Branlard, G., Charmet, G., & Guillon, F. (2007). Wheat arabinoxylans: Exploiting variation in amount and composition to develop enhanced varieties. *Journal of Cereal Science*, *46*, 261–281.

Sternemalm, E., Höije, A., & Gatenholm, P. (2008). Effect of arabinose substitution on the material properties of arabinoxylan films. *Carbohydrate Research*, *343*, 753–757.

Warrand, J., Michaud, P., Picton, L., Muller, G., Courtois, B., Ralainirina, R., et al. (2005). Contributions of intermolecular interactions between constitutive arabinoxylans to the flaxseeds mucilage properties. *Biomacromolecules*, *6*, 1871–1876.

Wissbrun, K. F., & Dealy, J. M. (1999). *Melt rheology and its role in plastics processing—Theory and applications*. Dordrecht: Kluwer Academic.

Won, J., Onyenemezu, C., Miller, W. G., & Lodge, T. P. (1994). Diffusion of spheres in entangled polymer solutions: A return to Stokes–Einstein behaviour. *Macromolecules*, *27*, 7389–7396.